NOTICE CONCERNING COPYRIGHT RESTRICTIONS

Geology and a Working Conceptual Model of the Obsidian Butte (Unit 6) Sector of the Salton Sea Geothermal Field, California

Jeff Hulen[1], Denis Norton[2], Dennis Kaspereit[3], Larry Murray[3], Todd van de Putte[3], and Melinda Wright[3]

[1]Energy & Geoscience Institute, University of Utah, 423 Wakara Way, Suite 300, Salt Lake City, UT 84108
Telephone 801-581-8497 e-mail *jhulen@egi.utah*
[2]Geologist/Geochemist, P.O. Box 310, Stanley, ID 83278
[3]CalEnergy Operating Company, 7030 Gentry Road, Calipatria, CA 92233

Keywords

Salton trough, Salton Sea geothermal system, lithology, structure, alteration, mineralization, breccia, veinlets, faults, fractures, geometry, magmatism, volcanism, rift, heat source, porosity, permeability, thermal-fluid flow, exploration guides, dilational microbreccia, calcite dissolution, epidote, specular hematite

ABSTRACT

A working conceptual model has been developed for the southwestern portion of the Salton Sea geothermal system, the region encompassing CalEnergy Operating Company's imminent "Unit 6" field expansion (185 megawatts). The model is based on examination and analysis of several thousand borehole rock samples combined with a wealth of subsurface information made available for the first time from the databases of present and prior field operators.

The Unit 6 sector of the system is hosted by fluvial and lacustrine, siliciclastic sediments and sedimentary rocks of Quaternary age. These strata are gently folded and cut by high-angle fault zones with a component of strike-slip displacement. The thicker of these zones (1) are mineralized and enriched in gouge and crush breccia (both commonly slickensided) as well as dilational microbreccia with a "jigsaw-puzzle" texture; and (2) are hosts for the most productive thermal-fluid conduits yet encountered in this part of the field. Much of this production is derived from major faults apparently forming the upper portion of a "negative flower structure", a common feature of transtensional wrench-fault regimes like the one in which the field is situated.

A unique, ~100-200 m-thick, evaporitic anhydrite-rich layer in the mudstone capping the sedimentary sequence is continuous except above the faults most productive at depth. We believe that only these faults penetrate significantly upward into the cap, providing ingress for cooler, sulfate-dissolving waters from above.

Unit 6 as drilled to date shares numerous attributes with the broader Salton Sea geothermal resource. The production fluids are hypersaline brines (total dissolved solids content 20-25%) circulating at temperatures generally in excess of 290°C. Porosity and permeability for fluid flow and storage are provided primarily by fractures, breccias, and veinlets, but also, in the upper part of the reservoir (and in a supra-reservoir outflow plume), by porous sandstones in which calcite has been hydrothermally dissolved. Overlying strata have not only retained their calcite, but have been mineralized locally with intergranular anhydrite, therefore providing an effective reservoir cap.

In addition to a paucity or absence of calcite, the following hydrothermal features are closely correlated with the Unit 6 geothermal reservoir: (1) pervasive veinlets of various compositions; and (2) widespread and commonly abundant epidote, accompanied locally at deeper levels by actinolite and clinopyroxene. The most prolific thermal-fluid channels coincide with fault-controlled concentrations of veinlets and dilational breccias mineralized with post-calc-silicate specular hematite ± anhydrite.

The foregoing observations and deductions are consistent with a conceptual geothermal reservoir centered above a still-cooling granitic pluton at least 2 km in diameter and ~3.5 km below the modern ground level. Major zones of buoyantly upwelling hot brine above the intrusion are focused along faults. More diffuse upflow occurs in a stockwork of interconnected, mineralized fractures (veinlets). This stockwork probably formed by hydraulic rock rupture induced by explosion of isolated, fluid-filled pores heated and consequently overpressured at an expanding (prograde) thermal front emanating from the magmatic heat source. Subhorizontal stratigraphic permeability in this model is concentrated in the upper portion of the reservoir, where the balance between carbonate dissolution and calc-silicate mineralization has favored formation of sandstone aquifers. Local downflow and warming of initially cooler brine from below the cap along major faults leads to slight (5-10°C) cooling of the upflow concomitant with open-space hematite ± anhydrite mineralization.

The Unit 6 geothermal reservoir is clearly open at depth and for at least a kilometer to the northwest. It extends to the southwest and (especially) to the northeast for considerably greater distances. The reservoir plunges abruptly to the southeast, but even here, by analogy with the northern part of the geothermal field, there is a high probability for encountering productive reservoir rock at

depths below 2 km. Our conceptual model, coupled with documented reservoir behavior here and elsewhere in the field, strongly suggests that the immediate resource is more than sufficient to support the planned expansion.

Introduction

The Energy & Geoscience Institute and CalEnergy Operating Company are collaborating to produce a new conceptual model of the Salton Sea geothermal field (SSGF), in the Imperial Valley of southernmost California (Figure 1). This famous field has been the site of numerous such modeling efforts in the past (Dondanville, 1966; Irvine, 1983; Suemnicht et al., 1984; Kasameyer et al., 1984; Mrlik and Strobel, 1986; Moore and Adams, 1988; Williams and McKibben, 1989; Butler and Schriener, 1991; Carrier, 1992; McKibben and Hardie, 1997; Schriener, Jr., 2001). The models have guided the operators in minimizing the risks and costs of field exploration and development.

CalEnergy, now the field's sole operator, has selected the Salton Sea resource for the country's largest field expansion in decades. The new "Unit 6" development, in what we will term the Obsidian Butte sector of the field (Figure 2), will add, with a single power plant, another 185 megawatts (MW_e) of electrical generation capacity to the existing 335 MW_e. The expansion will help strengthen the nation's energy security while bolstering the local tax base and providing well-paying jobs for the residents of Imperial County.

The Unit 6 expansion (and others almost certain to follow) will require dozens of deep new production and injection wells. A refined conceptual model for this part of the field is mandated if CalEnergy is to site and steer the wells to intersect the most productive reservoir rock with optimum efficiency and profitability. In this paper, we build upon the efforts of prior investigators to construct a provisional conceptual model combining relevant field-wide characteristics of the SSGF with site-specific attributes of the Unit 6 sector.

Geologic Setting

The Salton Trough, a major transtensional basin in southernmost California and northern Mexico (Figure 1), is the structural and physiographic extension of the Gulf of California (Elders et al., 1972; Elders, 1979; Lonsdale, 1989). The Gulf and the Trough straddle a transitional, plate-bounding rift zone separating the Pacific plate, to the west, from the North American Plate, on the east. Subsiding "pull-apart basins" (a type of spreading center) scattered along the length of the rift host vigorously active magma-hydrothermal systems. Two of these systems in the Trough, at Cerro Prieto and the SSGF (Figure 1), are among the world's largest and hottest. One well at the western edge of the SSGF encountered temperatures of at least 393°C at a depth of only 2 km (Hulen et al., 2002).

The Salton Trough began its existence in Oligocene to Miocene time as a coaxial but smaller and shallower proto-rift, developed as a Basin-Range-style back-arc basin in response to subduction of the Farallon plate beneath the North American plate (Karig and Jensky, 1972; Herzig and Jacobs, 1994). Oligocene to Miocene basalts along the margins of the modern Trough attest to the lithospheric thinning, heating, and mafic-alkaline magmatism that accompanied the older rifting episode (Herzig and Jacobs, 1994).

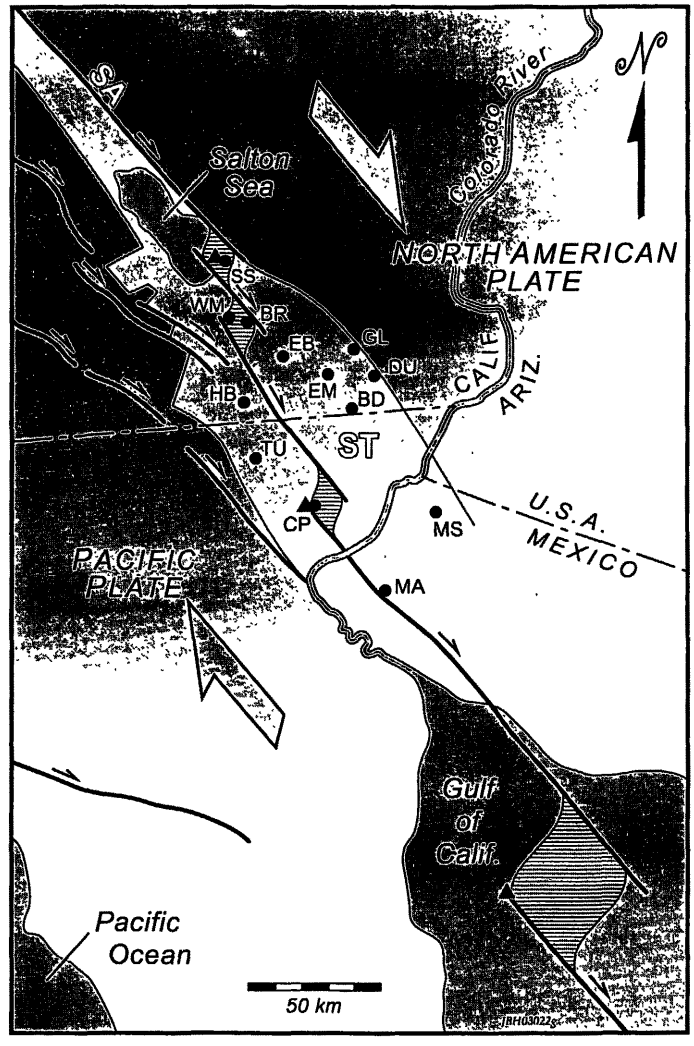

Figure 1. Location and tectonic map of the Salton Trough (ST) and its high-temperature geothermal systems relative to the southeastern terminus of the San Andreas transform fault zone (SA) and the northern tip of the Gulf of California. Geothermal fields (not all currently producing) abbreviated as follows: BD – Border; BR – Brawley; EB – East Brawley; EM – East Mesa; GL – Glamis; HB – Heber; MA – Mesa de Andrade; MS – Mesa de San Luis; SS – Salton Sea; TU – Tulecheck; WM – Westmoreland. Large arrows show modern relative motion of tectonic plates. Figure reproduced from Hulen et al. (2002). Synthesized and redrawn from Elders et al. (1979); Lachenbruch et al. (1985); and Elders and Sass (1988).

The modern Trough started to form between 4 and 5 Ma (Elders et al., 1972; Crowell, 1974; Lonsdale, 1989), as the proto-rift was further extended and ultimately ruptured to the asthenosphere to create a more landward margin between the North American and Pacific plates. The new plate boundary has evolved as a series of right-stepping, right-lateral transforms, linked at the oversteps by mantle-rooted pull-aparts (Elders et al., 1972).

The Trough was filled as it subsided by sediments from the Colorado River, which constructed a transverse dam ("the delta") across the basin, effectively blocking further marine incursions. Thereafter, periodic diversion of the River exclusively into the Trough rather than the Gulf supplied enormous amounts of water and sediment. As a result, the modern Trough is filled by up to 6 km of siliciclastic, fluvial and lacustrine mudstone, siltstone, and sandstone (Merriam and Bandy, 1965; Muffler and Doe, 1968; van de Kamp, 1973; Fuis and Kohler, 1984; Herzig et al., 1988).

The nature of the basement in the Trough remains conjectural. Gravity and seismic data suggest that low-density (2.3-2.55 g/cm^3) sediments rest upon an intermediate-density (2.65 g/cm^3) basement extending to about 12 km depth. The intermediate basement, in turn, overlies a higher density (3.1 g/cm^3) layer extending to the base of the crust at about 23.5 km (Moore, 1973; Fuis and Kohler, 1984; Lachenbruch et al., 1985; Elders et al., 1984). This deep layer is inferred to be gabbro, added to the crust to compensate isostatically for the low-density sediments supplied from above. The intermediate crust permissibly could be (1) hydrothermally metamorphosed Trough-fill sediments (Muffler and White, 1969); (2) pre-Trough continental crust, thinned and sparsely intruded by gabbro; or (3) some combination of these end-member alternatives.

Heat sources for the high-temperature geothermal systems of the Trough have traditionally been envisioned as gabbroic (e.g. Elders, et al., 1984). We suggest that granitic heat sources cannot be ruled out (see also Hulen et al., 2002). For one thing, the few exposed Quaternary volcanoes in the Trough are exclusively felsic (Reed, 1975; Robinson et al., 1976), implying corresponding subsurface felsic magmas. Moreover, Hulen and Pulka (2001) have documented thick, extrusive rhyolites up to 1.6 km deep in several SSGF geothermal wells. Chemical characteristics of these deep rhyolites (Hulen, unpublished data) indicate that, unlike the field's exposed rhyolite domes (Herzig and Jacobs, 1994), the former are products of crustal melting. The presence of the deep rhyolites suggests (1) that magmatism and volcanism have been much more extensive in the Trough than the few exposed volcanoes would suggest; (2) that sizeable granitic plutons may occur at depth; and (3) that at least intermittent igneous and hydrothermal activity predate the current Salton Sea hydrothermal system, which the results of an earlier numerical-modeling study (Kasameyer et al.,1984) suggest could be no more than 3,000 to 20,000 yr. old.

From the surface to depths reaching perhaps 6 km, the interior of the Salton Trough is filled by a thick sequence of Pliocene to Holocene, Colorado-River-derived, fluvial and lacustrine mudstones, siltstones, and sandstones. Based on examination of cores and cuttings from scientific well State 2-14, in the northern part of the SSGF, Herzig et al. (1988) concluded that thicker mudstone intervals in the sequence represent long-lived lakes, perhaps much like the modern Salton Sea. These authors also recognized sandstones deposited on lacustrine beaches and offshore bars, and in distributary-channel environments at various scales. Van de Kamp (1973) described similar depositional environments for Holocene Trough-fill sediments north of the Salton Sea.

Elders (1979) concluded that formation of large lakes has been a common phenomenon in the Salton Trough ever since the feature's inception. Stratigraphic and mineralogic evidence indicates that many of these lakes evaporated to dryness, in the process leaving extensive saline residues. Dissolution of these salt pans (e.g., Sykes, 1937) has been cited as an important source of solute for the Trough's widespread basinal brines (Elders, 1979; Rex, 1983, 1985; Osborn, 1989; McKibben and Hardie, 1997), including the evolved, high-temperature production fluids of the SSGF.

All thermal fluids in the SSGF are saline by global geothermal standards, but Williams and McKibben (1989) determined that the fluids have a crude vertical salinity (and therefore density) zonation. Deeper brines, generally below depths of about 1000 m, are exclusively hypersaline (20-34 wt.% total dissolved solids/TDS; Williams and McKibben, 1989; CalEnergy well files). Shallower brines above these depths range in TDS down to a few per cent. The brines are metalliferous (McKibben and Hardie, 1997), and have been responsible for generally weak but widespread base-metal mineralization (e.g., McKibben and Elders, 1985).

Methods and Procedures

Our approach in constructing a conceptual model for Unit 6 has involved application of a mix of traditional and novel research

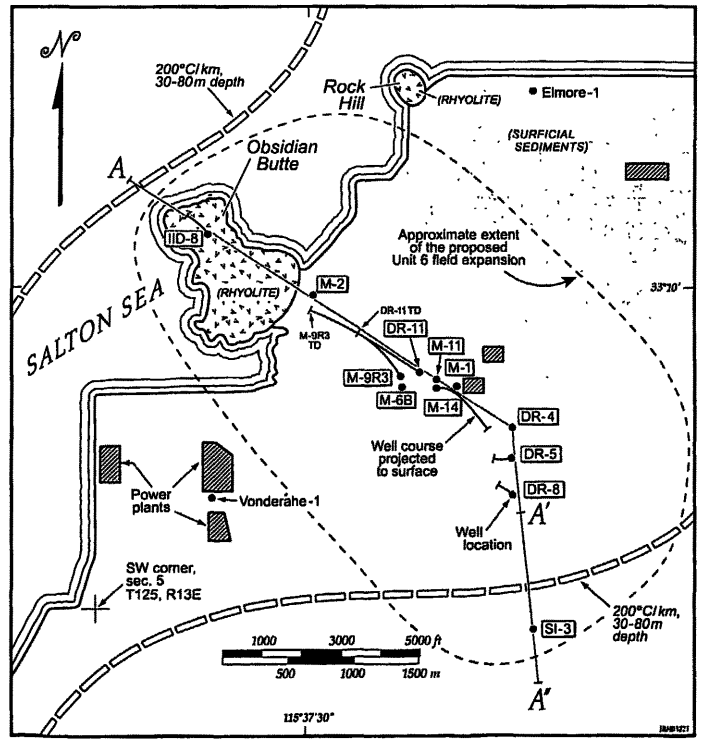

Figure 2. Map of the southwestern Salton Sea geothermal field, showing: (1) approximate extent of the 185 MW_e Obsidian Butte (Unit 6) expansion; and (2) geothermal wells utilized for this investigation. Margin of shallow (30-80 m) thermal anomaly above the field from Hulen et al. (2002) as modified from Newmark et al. (1988).

methods to comprehensive borehole sample suites, well logs, and reservoir-engineering data acquired by CalEnergy Operating Company and its predecessors, Unocal (Geothermal Division) and Magma Geothermal Company. All cuttings (more than 3,000 individual samples spanning 3.1-9.2 m intervals) and rare core samples from the study wells were first logged in detail, using a conventional binocular microscope, with emphasis on lithology, alteration, mineralization, and evidence of structural or other disruption. Representative samples were further examined petrographically, with support from X-ray diffraction, electron microprobe analysis, and scanning electron microscopy (results of the latter two investigations are deferred for a future paper). Compared judiciously with various geophysical well logs (e-logs), the resulting rock data were utilized to prepare a series of coincident 2-D geologic and mineralogic sections along a NW-SE transect through the proposed development (Figure 2). The geologic sections in turn were compared with corresponding static-temperature and thermal-gradient profiles, various reservoir-engineering data, and exploratory numerical modeling results (Norton) to conceptualize the pre-development state of the geothermal system.

By contrast with many prior geologic studies of the SSGF, our own relies more heavily upon actual borehole rock samples (principally cuttings) than e-logs. The rationale for the geophysical approach, routine for oil and gas exploration and development, has been that e-logs are superior to cuttings in representing an indigenous lithologic column. We disagree, and while we by no means discount e-logs for downhole geologic analysis, we also maintain that cuttings, studied with care and caution, yield a wealth of reliable and otherwise unobtainable direct subsurface information. Moreover, it is far from certain that e-log suites appropriate for low-temperature sedimentary stacks are equally applicable to similar sequences that are hot and hydrothermally altered. As one example, gamma-ray logs are traditionally used to help differentiate shales (and mudstones) from sandstones, as the former are generally more radioactive (Pickett, 1977). However, potassium-bearing minerals are the principal sources of this radioactivity. Sandstones in the Salton Sea geothermal reservoir are commonly enriched in hydrothermal adularia (potassium feldspar) and illite (potassium-rich micaceous clay), the two minerals along with quartz and calc-silicates entirely filling intergranular pores. Such mineralized sandstones conceivably could produce gamma-ray signatures otherwise more characteristic of shales.

A full discussion of the strengths and limitations of using drill cuttings for geologic analysis is beyond the scope of this paper; for detailed accounts, the reader is referred to Muffler and White (1969), Maher (1974), Tewhey (1977), and Hulen and Sibbett (1982). For our purposes, it is sufficient to note that with an un-

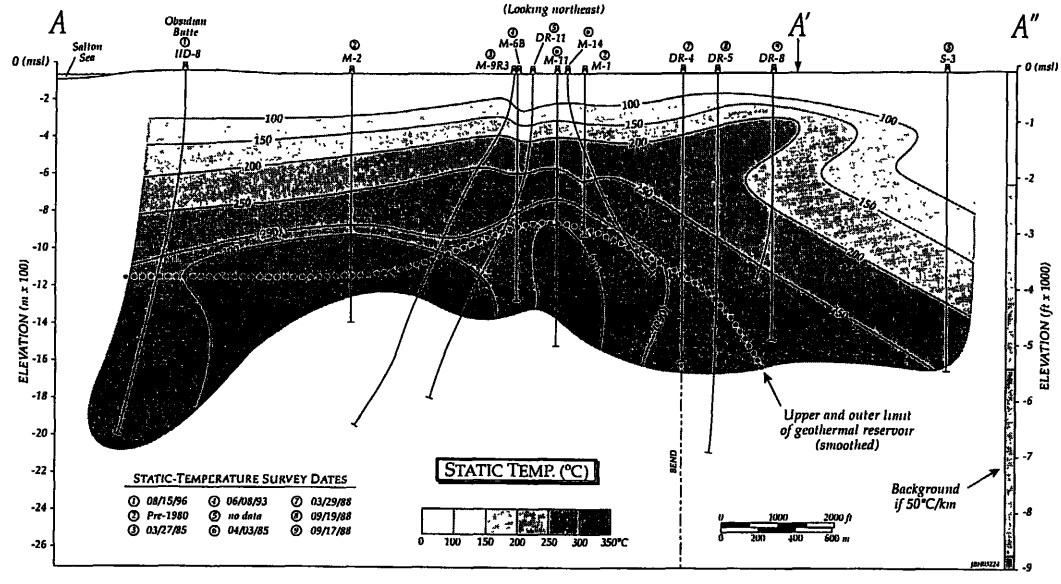

Figure 3. Static-temperature profile along the Unit 6 transect (section A-A"; see Figure 2 for location). Smoothed upper and outer limit of the geothermal reservoir (heavy dotted line) defined for this investigation as the approximate depth at which, above a temperature of ~275°C, static thermal-gradient profiles in the study wells (Figure 4) change from conductive (>50°C to ~1100°C per kilometer) to convective (<50°C to ~[-]200°C per kilometer).

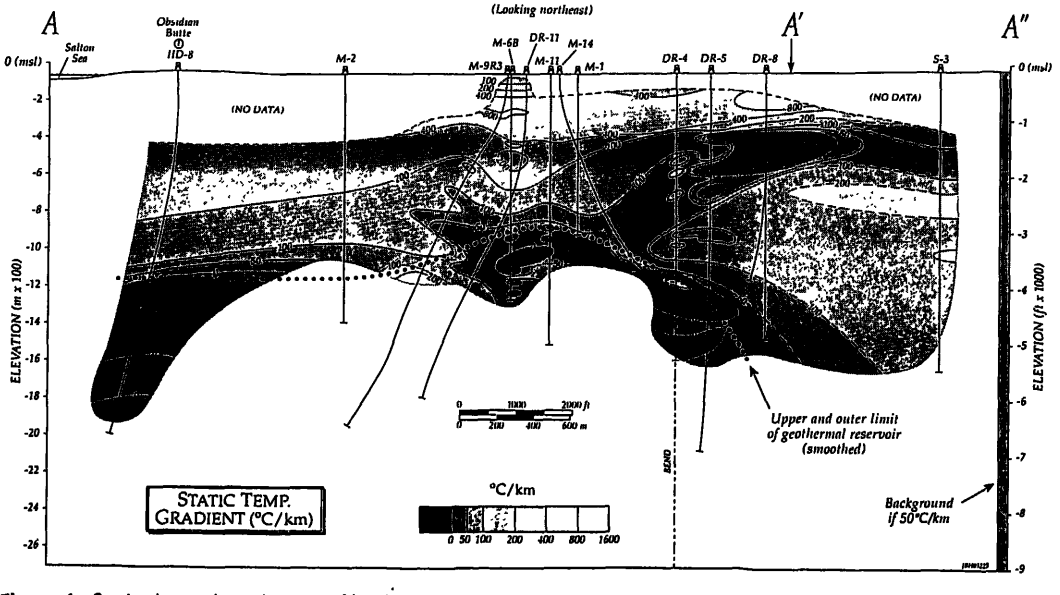

Figure 4. Static thermal-gradient profile along the Unit 6 transect (section A-A"; Figure 2).

derstanding of how cuttings are produced and collected, and how they can be contaminated, the potential pitfalls of the process can be minimized if not eliminated.

The Modern Geothermal Regime

The SSGF, including the Obsidian Butte sector, is confined to a broad, shallow thermal anomaly within which temperature gradients between 30 m and 80 m depth exceed 200°C per km (Figure 2; Kasameyer et al., 1984; Newmark et al., 1988; Hulen et al., 2002). This anomaly, about 72 km^2 in areal extent, is the near-surface expression of a vast magmatic-hydrothermal system circulating beneath an essentially impervious cap consisting of variously consolidated, calcareous siliciclastic sediments and sedimentary rocks. As defined by field operators, the top of the productive geothermal reservoir beneath this cap ranges in depth from less than 200 m to more than 1400 m.

We approximated pre-exploitation thermal conditions in Unit 6 by preparing coincident temperature and temperature-gradient profiles along the study section (A-A"; Figures 3 and 4). To construct these profiles, we utilized static-temperature logs acquired typically one to three months following completion of each of twelve wells (or deepenings thereof). The wells were drilled intermittently between 1974 and 1993 (with the majority completed between 1985 and 1988). Because of this lengthy time span, and because each well was put on line for production or injection soon after completion, there is clearly scope for artificial modification of natural-state (pre-development) temperatures and thermal gradients. We believe that any such production- or injection-induced changes have been trivial at most. To make this case, we refer the reader to the general similarity in static-temperature and thermal-gradient signatures of nearby wells M-1 (drilled in 1974) and M-6B (1993).

The top of the producing geothermal reservoir along the Obsidian Butte transect is defined here as the approximate depth at which, above a temperature of ~275°C (Figure 3), static thermal-gradient profiles in the study wells change from conductive (>50°C to ~1100°C per km) to convective (<50°C to ~[-]200°C per km) (Figure 4). At least 95% of the geothermal fluid from these wells is produced from below this interface. The maximum recorded static temperature along the transect is 317°C, just below the base of the cap in well M-9R3 (Figure 3).

The thermal-gradient section (Figure 4) shows several low-gradient lobes projecting above the geothermal reservoir upward and outward into higher-gradient surroundings. The most prominent of these lobes extends to the south in the upper reaches of wells DR-4, DR-5, DR-8, and S-3; others reach upward to the northwest from well DR-11 into the rocks of well M-9R3. We interpret these features as localized, pre-development, thermal-fluid upflow and outflow plumes.

Fluids produced from the study wells are concentrated Na-Ca-Cl brines with TDS in the range 20-25%. The brines are all derived from below production casing points (300-800 m depth), and are composite samples integrating multiple feed zones. Contributions from shallow, lower-salinity fluids such as those documented by Williams and McKibben (1989) cannot be ruled out. However, the high salinities of the composite samples indicate that deeper reservoir brines are by far the dominant constituents.

Geology of the Unit 6 Transect

The high-temperature geothermal system circulating in Unit 6 occurs in the upper third of the six-km-thick Salton Trough sedimentary sequence. Sediments and sedimentary rocks here are gently folded and cut by numerous high-angle fault zones, many of which apparently have a component of strike-slip displacement. The faulted strata are intruded sparsely by diabase, and overlain locally by Quaternary rhyolite. Hydrothermal alteration and mineralization of the sedimentary sequence grade downward from minimal at higher elevations to intense within the geothermal reservoir. Porosity and permeability in the reservoir are controlled by a combination of intergranular dissolution pores, fractures, veinlets, and dilational microbreccias. Fault-related, mineralized concentrations of the latter three features are strongly correlated with the most productive thermal-fluid entries.

Sedimentary Rocks

The sedimentary sequence penetrated by our study wells (Figure 5) encompasses the Brawley and uppermost Borrego Formations (Dibblee, 1954). The former unit, of Pleistocene to Holocene age, is dominated by a 350 to 400 m-thick, evaporite-

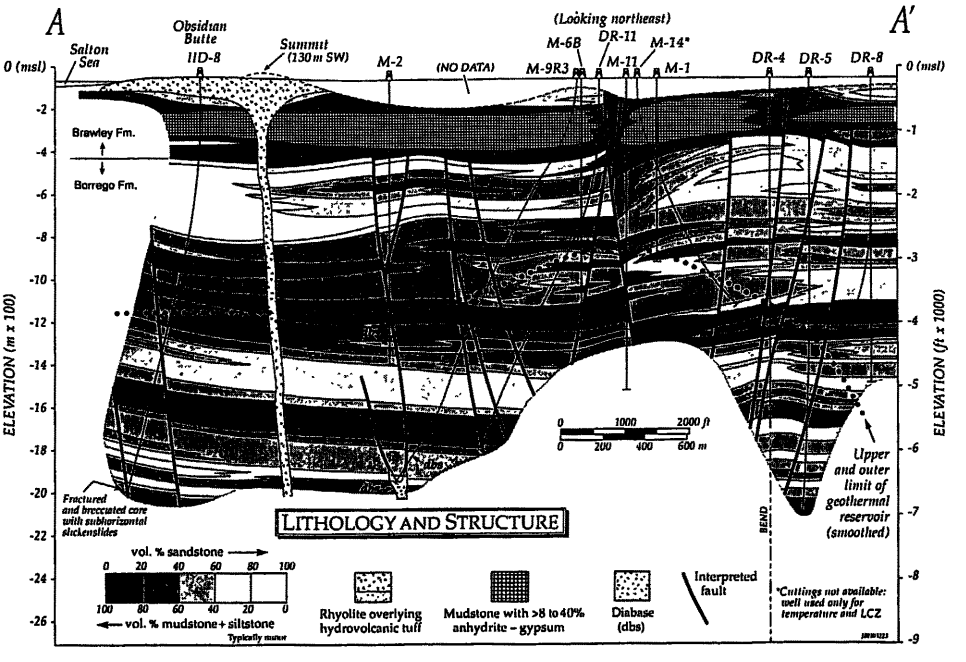

Figure 5. Geologic section along the Unit 6 transect (section A-A'; Figure 2; cuttings not available for well S-3). Constraints for the section provided by: (1) examination and analysis of drill cuttings; (2) location of lost-circulation zones; (3) location of thermal-fluid entries and injectate-exit points from temperature-pressure-spinner surveys; (4) dip angles from dipmeter logs; (5) other e-log signatures (locally, and judiciously weighted with respect to data from the other sources mentioned).

bearing, semi-consolidated, lacustrine mudstone (see also Tewhey, 1977). This ductile horizon serves as an effective natural cap on the geothermal system. The underlying upper Borrego Formation (Pleistocene) consists of interstratified, texturally and compositionally monotonous mudstones, siltstones, and sandstones like those encountered throughout the SSGF (e.g., Muffler and Doe, 1968; Helgeson, 1968; Younker et al., 1982) and cored in scientific drill hole State 2-14 (Elders and Sass, 1988; Herzig et al., 1988). Herzig et al. (1988) concluded from primary structures and bedforms in the State 2-14 cores that the sediments accumulated in a fluvial-lacustrine-deltaic depositional environment, with abrupt lateral and vertical facies changes the rule rather than the exception. With rocks like these, it can be problematic to correlate a single stratum between one well and its neighbor, let alone from one end of the study section to the other.

Accordingly, we developed a "pseudostratigraphy" for the Obsidian Butte transect, based on the relative percentages (in increments of 20%) of mudstone plus siltstone vs. sandstone for 18.3-m composite cuttings samples (Figure 5). This approach clearly defined the mudstone-dominated Brawley Formation cap, and revealed fair to excellent well-to-well correlation for sandstone- and mudstone-rich intervals of the underlying upper Borrego. Northwest of borehole DR-11, numerous pseudostratigraphic horizons in the deeper formation can be traced laterally through five wells over a span of two kilometers. A few of these horizons appear to persist southeastward beyond DR-11 (Figure 5), but the sequence here contains many more sandstone bodies of apparently limited lateral continuity.

Sandstones of the study section are typically very fine- to fine-grained, quartz-rich, and subarkosic to lithic-arkosic according to the classification of Folk (1968; see also Scholle, 1979). Where unaltered, the sandstones are typically buff-white to very light gray-buff, sparsely to abundantly micaceous, variably argillaceous, and commonly cemented by diagenetic calcite. In the Brawley Formation cap and uppermost underlying Borrego Formation, many of the "sandstones" are actually just accumulations of free sand grains. At higher elevations, this phenomenon can be ascribed to a lack of diagenetic cement. At deeper levels, hydrothermal calcite-dissolution appears to have liberated the grains.

Mudstones of the Brawley Formation are calcareous (>10% to 40% calcite), semi-consolidated, ductile, and change in color with depth from light grayish-orange through grayish-red to yellowish-gray. Smectitic clay, calcite, anhydrite, quartz, and feldspar in various combinations are the rock's principal constituents. Pure smectite at the top of the formation gives way gradually with depth to mixed-layer illite/smectite ± minor chlorite/smectite. Minor dolomite, ankerite, gypsum, chlorite, kaolin, pyrite; and terrigenous organic debris are also locally present. 1-3 mm-long gastropod and ostracod fossils occur sparsely in the upper 100 m of the formation, where the unit is relatively free of anhydrite and gypsum.

Borrego Formation mudstones are much more lithified than those of the Brawley Formation. Where comparatively unaltered, the Borrego mudstones are light to medium or dark gray to brownish-gray, well-consolidated, and moderately to strongly calcareous. The rocks consist dominantly of quartz, feldspar, illite, chlorite, and calcite, with lesser amounts of pyrite and black organic matter as well as scattered, <2-mm anhydrite nodules or their porous, calc-silicate-altered pseudomorphs (see also Osborn, 1989).

Siltstones in the Brawley and Borrego Formations are transitional in texture and composition between the mudstones and the very finest-grained sandstones. In either formation, the siltstones rarely account for more than a few percent of the total rock volume.

The Brawley Formation is unique along the study section in hosting a thick and laterally near-continuous evaporite layer (Figure 5). This horizon, spanning the approximate depth interval 200-350 m, contains 8-40% anhydrite, with minor local gypsum, encapsulated in semi-consolidated, yellowish-gray, ductile calcareous mudstone. The anhydrite is found principally as ovoid, white to gray, warty-surfaced, displacive diagenetic nodules up to 7 mm in diameter, but also as clearly laminated masses. The nodules grade downward in texture from chalky and microcrystalline to translucent and medium-crystalline. All but the microcrystalline nodules are characterized by an abundance of angular intercrystalline pores, which we speculate may initially have contained more soluble salts. Gypsum accompanies anhydrite toward the top of the evaporite, the hydrous sulfate occurring as crudely faceted, lens-like crystals up to 10 mm in diameter and invariably rimmed to partially replaced by anhydrite. Both the gypsum and anhydrite commonly are sparsely coated and/or intergrown with microcrystalline pyrite, determined elsewhere in the SSGF by Osborn (1989) to be the product of bacteriogenic sulfate reduction.

Igneous Rocks

Rhyolite and diabase are the only igneous rock types encountered along the study section (Figure 5); there are no intermediate-composition varieties. The rhyolite is confined to the Obsidian Butte flow-dome-tuff complex (Robinson et al., 1976), penetrated by well IID-8. The complex consists of glassy to stony, dark gray to pinkish-gray, sparsely porphyritic, flow-banded and peripherally pumiceous to perlitic rhyolite that overlies apparently massive tuff. The tuff contains blocky glass and pumice shards admixed with mudstone and sandstone lithic clasts in a nondescript but muddy microcrystalline matrix. The mudstone and shards are commonly clumped together in crudely ovoid, accretionary lapilli up to 5 mm in diameter. These lapilli and the blocky shards provide evidence that the tuff is of phreatomagmatic origin (Fisher and Schmincke, 1984; Wohletz, 1986), that is, it was produced by a steam explosion caused by the interaction of ascending felsic magma with shallow groundwater or perhaps an ephemeral lake like the Salton Sea

Diabase, found deep in wells M-2 and M-9R3 (Figure 5), is finely crystalline and consists principally of clinopyroxene and plagioclase with minor sphene, magnetite, and a variety of high-temperature hydrothermal minerals. The diabase is far less altered than enclosing sedimentary rocks. In thin section, the plagioclase in the intrusive is seen to be nearly fresh, and two-thirds of the clinopyroxene appears pristine. These relationships suggest that the mafic magma intruded an already well-established hydrothermal system.

Structure

Converging evidence indicates that the initially flat-lying Brawley and uppermost Borrego Formations along section A-A″

have been gently folded but extensively fractured and otherwise disrupted along high-angle faults (Figure 5). The folding is deduced from a combination of dipmeter data and correlation of pseudostratigraphic horizons from well to well. The faulting is based on synthesis and weighting of multiple criteria: (1) apparent offsets of pseudostrata between wells; (2) indigenous, commonly slickensided gouge and crush breccia [as opposed to "bit gouge" created by the drilling process] in cuttings; (3) major thermal-fluid entries and injectate-exit points determined from temperature-pressure-spinner surveys; (4) anomalous concentrations of veinlets and veinlet fragments [mineralized fractures] in cuttings; (5) lost-circulation zones; (6) abrupt vertical changes in dip angle from dipmeter logs; and (7) anomalous responses (e.g., chaotic acoustic signatures) on other e-logs.

The faults thus interpreted along the transect are high-angle and of only modest apparent dip-slip displacement, except for the steeply-southeast-dipping major break extending to depth beneath well DR-11 (Figure 5) in the approximate center of the section. The faults also show apparent down-dip displacement reversals (Figure 5). This geometry is characteristic of strike-slip or oblique-slip faults such as those of the San Andreas system along the eastern margin of the Salton Trough north of the SSGF (Sylvester, 1988).

The major structural disruption along the transect is clearly the central fault zone. Based on the northeast-southwest orientation of the associated upward bulge in the geothermal reservoir (Figure 5; Hulen et al., 2002; Hulen, unpublished top-of-reservoir map), we interpret this structure as an antithetic, left-lateral, strike-slip or oblique-slip fault in the prevailing, right-lateral, San Andreas-style wrench-fault regime. Susidiary high-angle faults southeast of the central zone dip northerly; those to the northwest dip to the southeast (Figure 5). All of these faults show minor dip-slip displacement. Accordingly, the main and subsidiary faults could be interpreted as being in the upper portion of a negative flower structure, another common feature in transtensional wrench-fault zones (Sylvester, 1988). One such flower structure in the nearby Mesquite mining district, about 60 km east of the SSGF, hosts a fossil hydrothermal system that for a time, at 2.3M troy ounces, was California's second-largest gold deposit (Willis and Tosdal, 1992).

Dilational Microbreccia– Chips of mineralized dilational microbreccia occur in association with gouge, crush-breccia, and slickensided cuttings in all of the study wells, but are particularly abundant in the lower portions of wells M-6B (Hulen et al., 2003), M-11, and IID-8 (Figure 5). These breccias are also associated with the most vigorous thermal-fluid entries along the transect, a relationship indicating that the breccias' geometry, distribution and abundance can provide valuable guidance for the siting and orientation of production and injection wells.

The dilational microbreccias consist typically of 0.1-1 mm-diameter angular clasts of altered siliciclastic rock and older vein material with an "exploded" or "jigsaw-puzzle" appearance, in which individual clasts commonly can be traced to their points of origin with little or no rotation. Although occurring with gouge and slickensides, the breccias themselves show no evidence of crushing, granulation, or shearing. The texture of the breccias in this geological environment (transtension, strike-slip faulting, and high-temperature fluid flow) suggests that the rocks originated by a combination of hydrothermal explosion (Grindley and Browne, 1976; Knapp and Knight, 1977) and implosion in dilational jogs along wrench faults (Knapp and Knight, 1977; Sibson, 1986; Hulen et al., 2003).

Alteration and Mineralization

The high-temperature, metalliferous brines of the Salton Sea geothermal system have interacted with their host rocks to produce well-zoned secondary-mineral assemblages that have been used by numerous prior investigators to assess the system's configuration and evolution (e.g., White et al., 1963; Skinner, 1967; Helgeson, 1968; Muffler and White, 1969; Bird and Norton, 1981; McDowell and Elders, 1983; Kasameyer et al., 1984; McKibben and Elders, 1985; McKibben et al., 1987,1988; Caruso et al., 1988; Charles et al., 1988; Williams and McKibben, 1989). Our approach builds upon but differs from these investigations in several ways: (1) The number of wells and samples (respectively, a dozen and several

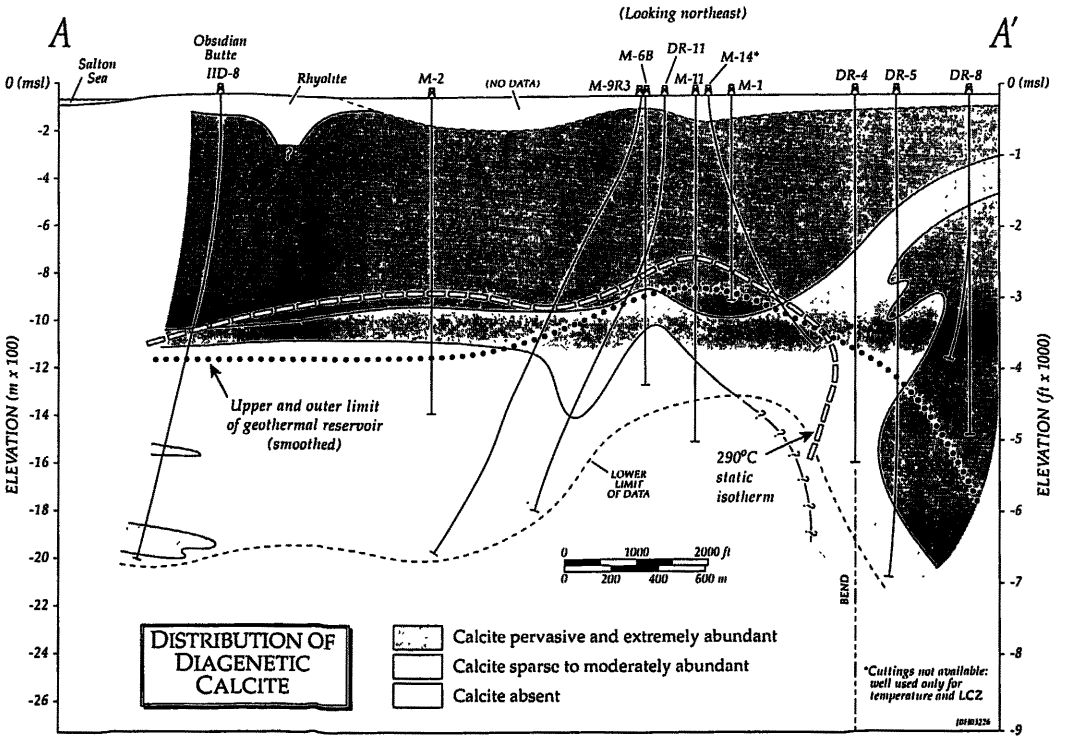

Figure 6. Distribution of diagenetic calcite in drill cuttings along the Unit 6 transect. Note essentially antithetic relationship between calcite and the high-temperature geothermal reservoir.

thousand) together employed for the study is unprecedented; (2) All samples were examined and analyzed in detail, providing a voluminous and continuous record of alteration, mineralization, and secondary-mineral paragenesis along the section; (3) The investigation is focused on finding new ways to locate and map the most productive reservoir rocks and thermal-fluid channels at depth; and (4) It is geared toward developing easy-to-use mineralogical and textural reservoir guides for the on-site personnel actually involved in defining and producing the resource.

Dissolution and Replacement of Calcite – There is a generally inverse relationship along the Obsidian Butte transect between the geothermal reservoir and the abundance of diagenetic and other forms of calcite (Figure 6, previous page). Above and lateral to the reservoir, calcite occurs in abundance as a diagenetic cement and sparsely as detrital grains. A few veinlets of the carbonate also occur in the rocks flanking the reservoir to the southeast. Within the reservoir, calcite of any variety is typically sparse to absent.

Textural and mineralogical relationships indicate that the paucity or absence of calcite within and just outside the reservoir is the coupled result of the carbonate's hydrothermal replacement by calc-silicates and its wholesale hydrothermal dissolution. The relative effects of these processes vary with location. In the upper and outer reservoir and its flanks, dissolution has dominated and intergranular porosity has been enhanced. Deeper in the reservoir, calc-silicate replacement has prevailed over dissolution, and has been accompanied by open-space precipitation of quartz, adularia, albite, and other hydrothermal phases. In this fashion, intergranular porosity has actually been reduced. Deep-reservoir porosity and permeability appear to be controlled principally by faults, fractures, breccias, and veinlets.

Note that the prominent outflow plume defined by static temperatures and temperature gradients in the upper portions of wells DR-4, DR-5, and DR-8 (Figures 3 and 4) is mirrored by a calcite-deficient (but not absent) zone (Figure 6) in a sand-rich portion of the upper Borrego Formation. This zone is largely devoid of epidote or other calc-silicates, but is marked by chloritization and scattered base-metal mineralization (the cuttings from one 12.2-m interval within the plume in well DR-5 contain 2-4% chalcopyrite).

Dissolution and Reprecipitation of Anhydrite – Above an arbitrary concentration threshold (~8 v.% calcium sulfate), the thick, distinctive, Brawley Formation evaporite layer is continuous along the study section except in wells DR-11 and DR-4 (Figure 5). In these wells, the Brawley mudstones contain only a few percent anhydrite ± gypsum. This relative sulfate scarcity in the cap coincides with the upward projections of the central major fault zone (DR-11) and a subsidiary structure to the south (DR-4). We suggest that these faults may be the only ones along the section that effectively breach upward into the cap. Ephemeral open spaces created intermittently by renewed slippage on these structures may temporarily allow cool waters within the cap to percolate downward toward the geothermal reservoir. Since anhydrite has retrograde solubility, the cool waters initially would dissolve the newly accessible sulfate. With greater depth, heating of these downflowing fluids conversely would cause anhydrite to precipitate, thereby enhancing the reservoir cap (Moore and Adams, 1988).

Calc-Silicates – Hydrothermal calc-silicates identified to date along the Obsidian Butte transect are epidote, actinolite, and clinopyroxene. The latter two minerals occur deep in the geothermal reservoir and are generally scarce; their distributions are not plotted for this paper. Epidote is by far the most common, locally accounting for as much as 15 v.% (Figure 7). The mineral occurs not only as a replacement of original carbonate and other diagenetic and detrital minerals, but also as open-space linings and fillings of various origins. The greatest concentrations of epidote are confined largely to the calcite-free zone, in which the mineral is strongly correlated with sandstone abundance (Figures 5 and 7). The interpreted distribution of epidote accordingly has a distinctly stratiform appearance.

Layer Silicates – The distribution of secondary layer silicates along the study section is much the same as documented by previous workers for other portions of the SSGF (e.g., McDowell and Elders, 1980). Pure smectite of diagenetic origin at the top

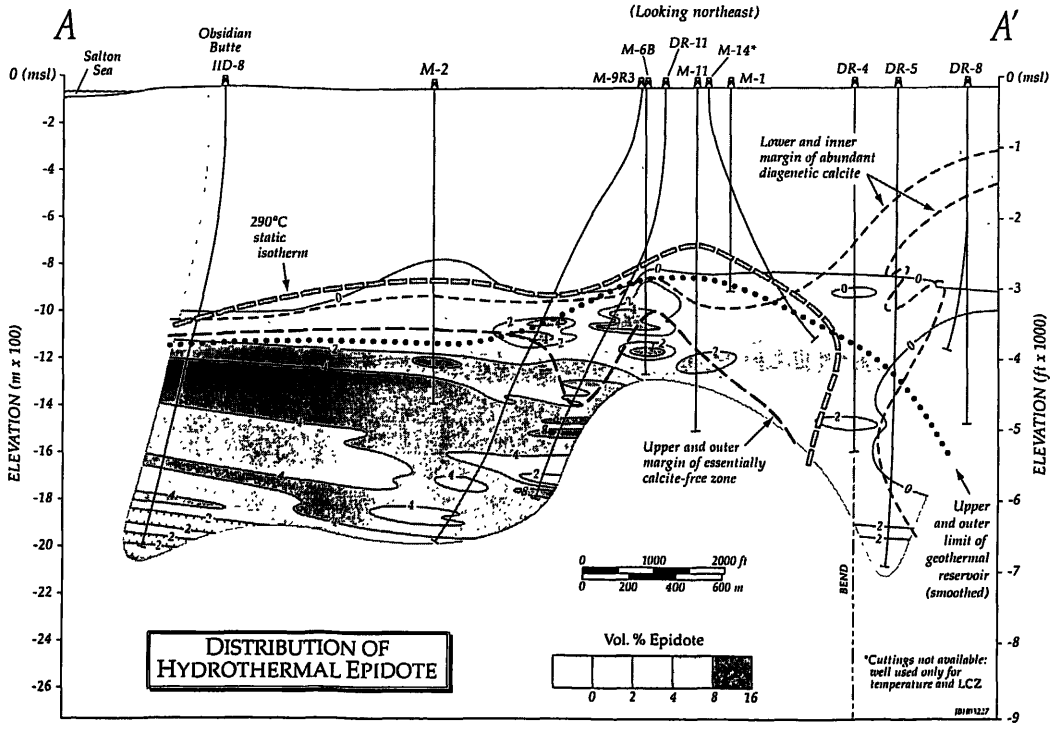

Figure 7. Distribution of hydrothermal epidote in drill cuttings along the Unit 6 transect. The epidote is strongly correlated with the geothermal reservoir, and coincides largely with the calcite-free and calcite-depleted zones (Figure 6). The calc-silicate is also strongly concentrated in sandstone-rich horizons, and its interpreted distribution accordingly has a stratiform aspect.

of the transect transforms with increasing depth and increasing temperature to mixed-layer illite/smectite and/or chlorite/smectite), then illite with no expandable interlayers. Secondary chlorite appears in approximate conjunction with the 240°C static isotherm (Figure 3), and secondary biotite is confined beneath the 300°C isotherm. Detailed discussion and illustration of layer silicate assemblages along the Obsidian Butte transect are deferred for future publication.

Sulfides – Sulfide minerals are conspicuous but minor constituents of the study-well cuttings. Pyrite is nearly ubiquitous from the shallowest to the deepest reaches of the wells. We have noted the occurrence of a bacteriogenic form of the iron sulfide in the anhydrite layer of the cap. Beneath the cap, pyrite accounts for a trace to one percent (rarely more) of most cuttings samples. It occurs as disseminated grains in all rock types; as scattered, probably syngenetic laminae in a few mudstones; and as a common constituent of hydrothermal veinlets. The base-metal sulfides chalcopyrite, sphalerite, and galena (in descending order of abundance) are much more local in distribution than pyrite; do not form syngenetic accumulations; and tend to be concentrated in the veinlets.

Hydrothermal Veinlets – Below a depth of about one km, and to the northwest of well DR-4, almost every cuttings sample from the study wells contains at least traces of hydrothermal veinlets or veinlet fragments (Figure 8). The veinlets are distinctive and texturally self-evident, discordantly cutting through individual drill chips. The veinlet fragments can be readily distinguished from disaggregated intergranular fillings/replacements and replaced framework grains because the fragments: (1) are generally tabular; (2) are larger (up to several mm) than could be accommodated by grains or intergranular space; and (3) commonly have drusy micro-crystals projecting either toward the open center of a fragment, or outward from one or both major surfaces.

The distribution of veinlets is strongly correlated with the geothermal reservoir (Figure 8). The most abundant veinlets occur in association with gouge and slickensides as well as crush and dilational microbreccias. These anomalous veinlet concentrations accordingly are interpreted as fault-controlled fracture fillings. Less abundant (tr.-2%) veinlets in the reservoir nonetheless occur ubiquitously along the transect over a vertical area of at least 3.5 km^2, forming what must be a stockwork of mineralized fractures that is unlikely to be of purely tectonic origin. Rather, we infer that the fractures formed when isolated, fluid-filled pores exploded in response to heating at an expanding thermal front emanating from a deeper magmatic heat source (Knapp and Knight, 1977).

Specular Hematite – Among all secondary minerals identified in the study wells, specular hematite is most closely associated with productive thermal-fluid entries. The oxide occurs primarily in hydrothermal veinlets (Figures 8 and 9), but also as breccia cements and sparse disseminations in sandstones. Vein- and breccia-hosted specular hematite, with or without anhydrite, quartz, chlorite, adularia, and pyrite (in descending order of abundance) in highly porous accumulations, accounts for up to 7% of the rock in the lower several hundred meters of wells M-6B and M-11 (Figure 9). As determined by analysis of pressure-temperature-spinner surveys, the hematite zone in the former well by itself yields enough thermal fluid to support an electrical-generation capacity of about 34 MW_e (Hulen et al., 2003).

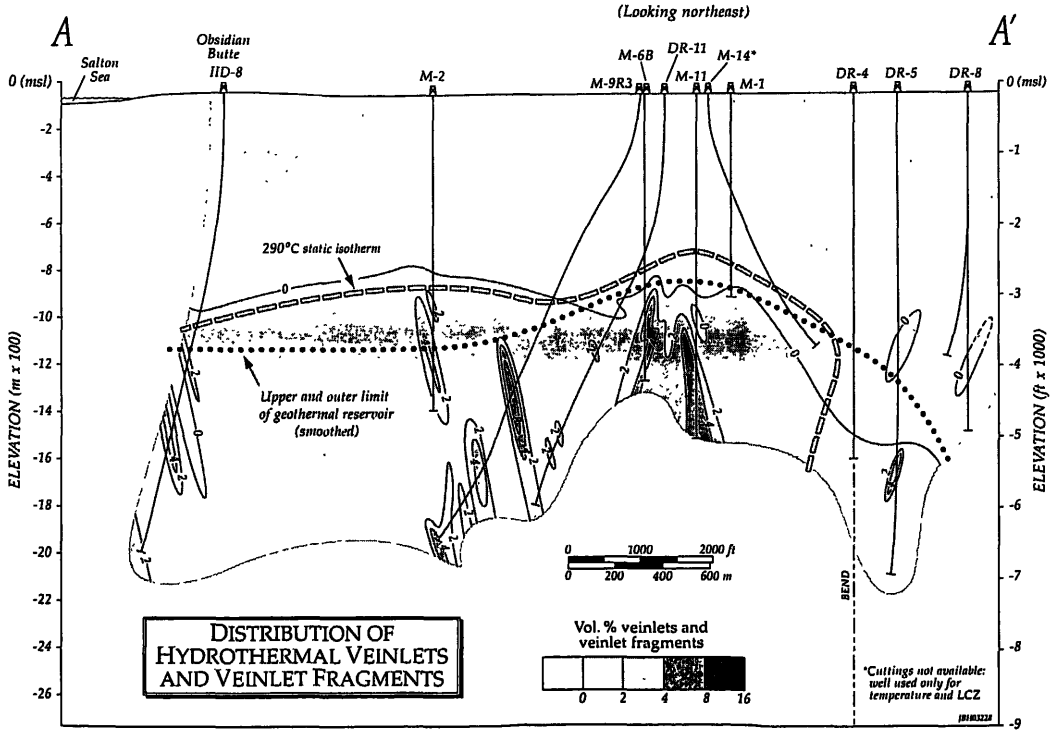

Figure 8. Hydrothermal veinlets and veinlet fragments in cuttings along the Unit 6 transect. The overall distribution of veinlets shows good correlation with the geothermal reservoir, but strong concentrations of veinlets are associated with fractures, faults, and breccias that we have interpreted as steeply-dipping features (Figure 5).

The Conceptual Model: Discussion and Conclusions

Essential components of an effective conceptual model for the Unit 6 hydrothermal system are as follows: (1) size; (2) geometry; (3) heat source; (4) thermal-fluid origin, composition, and evolution; (5) nature and extent of porosity and permeability; (6) location and vigor of upflow and downflow zones; (7) position and direction of inflows and outflows; and (8) mineralogical and textural zoning characteristics useful for mapping the system and for predicting approach either to productive thermal-fluid channels or to cooler conduits more suitable for injection. The evidence presented above, assessed in the light of prior investigations, allows us to address each of these elements and to present a working, 2-D conceptual model for further testing and refinement.

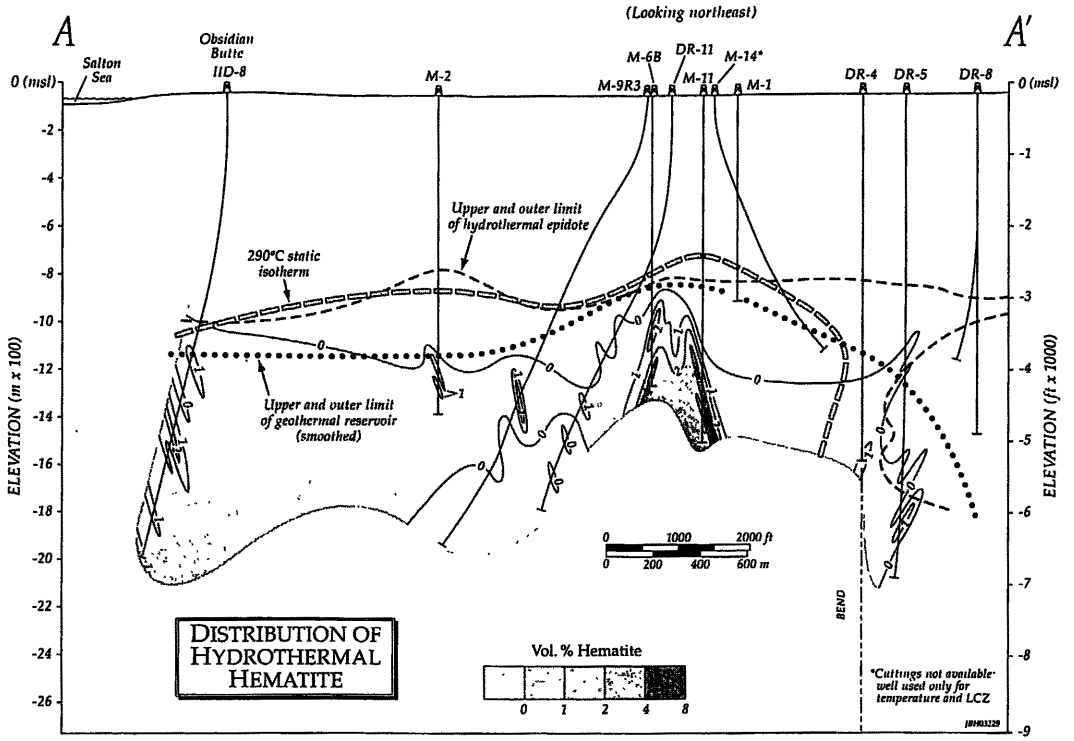

Figure 9. Distribution of hydrothermal specular hematite in cuttings along the Unit 6 transect. The hematite is confined largely to the geothermal reservoir and associated epidote zone, but is concentrated in veinlets and dilational microbreccias along interpreted fault zones. Anomalous concentrations of specular hematite, with or without hydrothermal anhydrite, are first-order guides to the most productive thermal-fluid channels.

Size

In two dimensions (a temporary limitation to our modeling efforts), the thermal anomaly along the study section is about 5 km wide and 2 km deep, for a minimum vertical areal extent of about 10 km^2 (Figure 3). The producing geothermal reservoir within that anomaly is about 3.5 km wide and 1 km deep (3.5 km^2). The margins of the thermal anomaly and reservoir plunge to the south, but there is clearly potential for deeper production below the bottom of well DR-8. This assertion is based on the fact that the top of the productive reservoir in the River Ranch (northeastern) part of the SSGF is commonly below 2 km depth (CalEnergy well-data files).

Both the thermal anomaly and geothermal reservoir along the transect are distinctly open to the northwest (Figure 3). The tops of the anomaly and the reservoir are apparently subhorizontal between wells M-2 and IID-8, and there is no indication that either feature at the northwestern end of the section is close to the point where it plunges. The reservoir in IID-8 is a few degrees cooler than in M-2. Based on this fact; on the presence of reservoir calcite; and on the relationship of the reservoir to the overlying shallow thermal-gradient anomaly (Figure 2), we believe that (1) IID-8 is closer to the edge than the center of the reservoir; but (2) the producible resource extends to the northwest beyond the end of the section for at least another kilometer.

The maximum depth of the reservoir is conjectural, but there is no reason to assume that drilling to date has tested this limit. Core from the bottom of well IID-8 (Figures 5, 8, and 9), for example, is porous, fractured, brecciated, and mineralized in the same fashion as cuttings from the section's most prolific production zone (in the lower reaches of well M-6B). The bottom of IID-8, 2 km deep, was also a massive lost-circulation zone and is believed to host a major thermal-fluid entry. It is virtually certain that productive reservoir rock extends considerably below this depth.

Geometry

The 2-D configuration of the Unit 6 geothermal reservoir as drilled to date reflects a combination of stratigraphic and structural controls. Based on available data, the top of the northwestern half of the reservoir is interpreted as relatively flat-lying, mimicking the attitude of the sedimentary host rocks and cap (Figures 3 and 4). The top of the southern half of the reservoir bulges upward, cutting across stratigraphy. The steeply plunging southeastern margin of the resource is similarly discordant, and both features are clearly related to thermal-fluid upflow along major high-angle fault zones. Lobes of high-temperature and (especially) low-thermal-gradient rock projecting upward and outward from the reservoir (Figures 3 and 4) likewise follow faults and stratigraphic aquifers.

Heat Source

As noted in the "Geologic Setting" section of this paper, mantle-derived gabbros have generally been invoked as the immediate heat sources for high-temperature hydrothermal systems of the Salton Trough (e.g., Elders, 1984; McKibben et al., 1988; McKibben and Hardie, 1997). We cannot rule out a mafic heat source for Unit 6 (or, indeed, elsewhere in the SSGF), but suggest that a felsic heat source might be more likely. Our rationale for this suggestion can be outlined as follows: (1) In the drilled subsurface of the field, the aggregate thickness of felsic igneous rock is an order of magnitude greater than that of mafic igneous rock; and (2) most of the felsic rocks are extrusive rhyolites (Hulen and Pulka, 2001; Hulen, unpublished data), much like Obsidian Butte but larger, with volumes perhaps as much as several km^3. These voluminous rhyolites imply corresponding and probably larger granitic magma chambers. Such felsic chambers, unlike those of mafic composition, are prone to pond in large volumes in the upper crust (Smith and Shaw, 1975; Wohletz and Heiken, 1992), providing long-lived heat engines for the inevitably associated hydrothermal systems.

From the foregoing analysis, and based on a suite of graphical portrayals of generic and site-specific numerical magma-hydrothermal systems (e.g., Norton, 1979, 1982; 1984; Norton and

Hulen, 2001), we envision the heat source in our conceptual model as a cooling granitic pluton, about 2 km in width, with its top centered just southeast of the bottom of well M-2 at about 3.5 km depth (Figure 10). Still-molten pockets in this pluton conceivably could have been the sources of the felsic magmas that erupted to form the Obsidian Butte rhyolitic complex.

Thermal-Fluid Origin, Composition, and Evolution

The Na-Ca-Cl production brines from our study wells differ little compositionally from those sampled elsewhere in the SSGF (e.g., Helgeson, 1968). Nor at this point in our investigation is there any reason to modify existing models for the sources and high salinities of these brines. In various ways, the models feature Colorado River water: (1) dissolving surficial salt pans as well as deeper evaporite-rich beds, then sinking into the basin due to increased density; (2) gaining heat and becoming buoyant above cooling plutons; and (3) acquiring metals and additional solutes by circulating through and interacting with siliciclastic strata of the Salton Trough sequence (Helgeson, 1968; Rex, 1983, 1985; McKibben et al., 1987; Williams and McKibben, 1989). Brines of different salinities produced by these processes locally mix and precipitate sphalerite, galena, and other base-metal sulfides (McKibben and Elders, 1985).

The composite, study-well brines, at 20-25 wt.% TDS, are only slightly less concentrated than their counterparts from deeper portions of the resource in the northern part of the field (26 to [rarely] >30 wt.%; Helgeson, 1968; CalEnergy well-data files). Other factors equal, the former would require less thermal input than the latter to become sufficiently buoyant to ascend. Contributions to the study-well reservoir brines from density-stratified, higher-elevation, lower-salinity (5-15 wt.% TDS) thermal fluids like those documented elsewhere in the SSGF (e.g., Williams and McKibben, 1989) are likely to be minor and local in Unit 6.

Porosity and Permeability

Published and proprietary studies of the SSGF differ in their views of the relative importance of stratigraphic/intergranular vs. fracture porosity and permeability. Proprietary accounts favor scenarios in which major discrete fault zones feed ascending thermal fluid into multiple porous sandstone bodies, the latter serving as the principal geothermal reservoir rocks (e.g., Butler and Schriener, 1984; Carrier, 1992). Published works largely dismiss stratigraphic effects, citing in support the fact that isotherms and brine interfaces in the field commonly transgress bedding. McKibben and Hardie (1997), for example, state that "the sediments hosting the brines have been metamorphosed to dense, fractured hornfels [which acts as a] homogeneous, porous medium for the brines".

Results of the present investigation demonstrate that along the Obsidian Butte transect, mineralized fractures and breccias, especially in major high-angle fault zones, provide the principal high-temperature thermal-fluid channels. Sandstone aquifers appear to be important only above, outside, and in the uppermost portions of the geothermal reservoir proper.

Textural and mineralogical evidence indicates that Unit 6 fracture zones providing the best thermal-fluid channels have developed as a result of coupled mechanical, thermal, and chemical effects. The governing processes are dilation and depressurization due to slippage at irregularities along faults (Sibson, 1986) together with hydrothermal rock rupture.

Hulen et al. (2003) cited evidence that mineralized fractures and breccias in the lower portion of well M-6B (Figures 8 and 9) formed in response to (1) implosion at a dilational jog along an antithetic, left-lateral strike-slip fault; abetted by (2) thermally-induced overpressuring and explosion of isolated, fluid-filled pores (Knapp and Knight, 1977). The latter process prevails only during the prograde phase of an evolving hydrothermal system, but

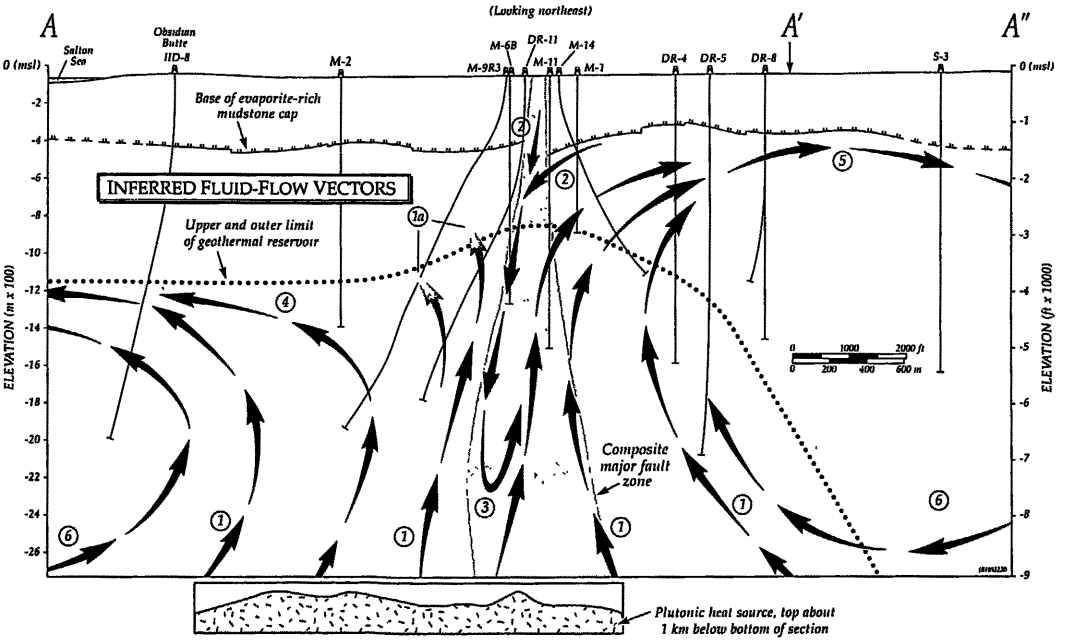

Figure 10. Provisional conceptual model of modern, natural-state (pre-development) thermal-fluid flow along the Obsidian Butte study section. Key components for the model include a ductile mudstone cap; a central major composite strike-slip fault zone; and a deep-seated plutonic heat source as well as the following numbered features: (1) Fracture-channeled, high-temperature (generally >300°C), thermal-fluid upflow, particularly copious along the central fault zone; (1a) such upflows exiting the plane of the section, probably to the southeast; (2) cooler (but still mostly >200°C) local downflow, induced by depressurization in dilational jogs created by renewed horizontal slippage along the fault zone; (3) re-ascent of the initial downflow, at the point where the gradually warming fluid has become sufficiently buoyant; (4) subhorizontal reservoir-flow channeled by sandstones in which intergranular porosity and permeability have been enhanced by hydrothermal calcite-dissolution; (5) outward-cooling, high-elevation outflow, also largely constrained to sandstone; (6) deep inflow to replenish the upwelling thermal plumes.

the pressure effects are enormous, in the range of 10-20 bars per degree Celsius of heating (e.g., Norton, 1984). Norton and Dutrow (2001; equations 7, 8, and 9) have demonstrated that pore-fluid overpressuring and rock rupture tend to reorganize and concentrate initially scattered pore space into elongate, veinlet-like forms that are ideal for transmitting thermal fluids. Whether or not these or any potential channels remain open also depends upon a favorable geochemical environment. In the M-6B fractures and breccias, an auspicious balance between open-space creation and mineralization has resulted in hematite ± anhydrite veinlets and breccia cements with up to 30% interconnected porosity (Hulen et al., 2003). These features are ideal thermal-fluid conduits, and account for much of the geothermal production along the Obsidian Butte transect.

Pore-fluid overpressuring and consequent hydraulic fracturing are also likely responsible for the broader zone of veinlets within which the hematite zones occur (Figures 8 and 9). These less abundant but pervasive veinlets are as common in mudstone as in sandstone, and their porosity ranges from nil to perhaps 30%. Because the veinlet stockwork correlates so well with the geothermal reservoir, we believe that the more porous veinlets: (1) account for much of the reservoir's permeability; and (2) provide channels through mudstones that might otherwise be aquicludes.

Sandstone aquifers within and above the geothermal reservoir are mostly those within which original calcite has been diminished or removed by hydrothermal dissolution. The best example of this phenomenon is the upward- and outward-reaching, low-thermal-gradient anomaly coinciding with calcite-depleted sandstones in the upper portions of wells DR-4, DR-5, and DR-8 (Figures 4-6).

Upflows, Downflows, Inflows, and Outflows

A provisional conceptual model of thermal-fluid flow within, above, and immediately adjacent to the modern geothermal system cut by the Obsidian Butte transect is shown as Figure 10. The model is based on the observations, measurements, and deductions presented earlier in this paper compared with a suite of published analyses and graphical portrayals of numerical magma-hydrothermal systems (Norton, 1979, 1982; 1984; Norton and Hulen, 2001).

In common with the model of Williams and McKibben (1989), our own begins with thermal energy dissipating from a young cooling pluton and heating brine in the overlying sedimentary sequence. These processes reduce the density of the brine relative to otherwise similar flanking fluids at the same elevations. The buoyant, lower-density brine ascends, both in fault-related fractures and in breccias and hydrofractures created during an earlier stage of the still-extant prograde thermal field. The upflows are compensated at depth by brine inflow from the margins of the system. Beneath and locally within a reservoir cap of unaltered to weakly altered and sparingly permeable sediments, the upflows are deflected outward, in part in sandstone aquifers created by dissolution of diagenetic calcite. Late-stage tectonic and hydraulic fracturing along major fault zones creates additional secondary permeability, permitting the downflow of cooler (initially about 200°C) brine mostly from just below the overlying, evaporite-rich mudstone cap. The downflowing brine heats as it descends, in the process depositing hematite ± anhydrite, but nonetheless reduces temperatures in the original upflow by several degrees Celsius. At a conjectural depth, the descending brine becomes sufficiently hot and buoyant that it reverses direction and joins the still-prevalent upflow regime.

Exploration and Development Guides

In the course of this investigation, we have discovered or confirmed a number of tectonically and/or hydrothermally induced textural and mineralogical features that will be useful during the Unit 6 expansion for targeting the most productive geothermal reservoir rock and thermal-fluid conduits.

- There is good correlation between the extent of the reservoir and the presence of epidote and absence or paucity of diagenetic calcite. These features signal potentially productive rock volumes, but there is no particular relationship between epidote abundance and thermal-fluid entries.
- On the other hand, the presence of dilational microbreccia and abundance of specular hematite (with or without hydrothermal anhydrite) are first-order guides to the location and size of these entries.
- The near-surface expression of the major fault zones most productive at depth may be dissolution-induced anhydrite depletion in evaporite-rich mudstone of the ductile Brawley Formation cap.

Acknowledgements

Hulen and Norton's participation in this research project is being funded by the U.S. Department of Energy, Office of Geothermal Technologies (Roy Mink, Program Manager), Grant No. DE-FG07-00ID13891. Said support does not necessarily constitute an endorsement of the work presented in this paper. We are grateful to Phil Messer, head of the CalEnergy Resource Group, and to MidAmerican Energy Holdings for permission to publish. Illustrations are the work of EGI graphic artist Doug Jensen.

References

Bird, D.K., and Norton, D.L., 1981, Theoretical prediction of phase relations among aqueous solutions and minerals, Salton Sea geothermal system: Geochimica et Cosmochimica Acta, v. 45, p. 1479-1493.

Butler, S.J., and Schriener, A., Jr., 1991, Unit 1-3 area reservoir model and preliminary simulation, Salton Sea reservoir: Unocal, Geothermal Division, Internal Report, 8 p.

Carrier, D., 1992, Full-field geologic conceptual model for the Salton Sea geothermal reservoir: Unocal, Geothermal Division, Internal Report, 86 p.

Caruso, L.J., Bird, D.K., Cho, M., and Liou, J.G., 1988, Epidote-bearing veins in the State 2-14 drill hole – Implications for hydrothermal fluid composition: Journal of Geophysical Research, v. 93, p. 13,123-13,133.

Charles, R.W., Janecky, D.R., Goff, F., and McKibben, M.A., 1988, Chemographic and thermodynamic analysis of the paragenesis of major phases in the vicinity of the 6120-foot (1866-m) flow zone, California State 2-14: Journal of Geophysical Research, v. 93, p. 13,145-13,157.

Crowell, J.C., 1974, Origin of late Cenozoic basins in southern California: Society of Economic Paleontologists and Mineralogists, Special Publication 22, p. 190-204.

Dibblee, T.W., Jr., 1954, Geology of the Imperial Valley region, California *in* Geology of southern California (R. H. Jahns, editor): California Division of Mines Bulletin, v. 170, p. 21-28.

Dondanville, R.F., 1966, Geology of the Niland (Salton Sea) geothermal area: Consulting Report for Earth Energy, Inc., 52 p.

Elders, W.A., 1979, The geological background of the geothermal fields of the Salton trough *in* Geology and geothermics of the Salton trough (W.A. Elders, editor): Geological Society of America, 92nd Annual Meeting, San Diego, California, Field Trip Guidebook for Field Trip No. 7, University of California, Riverside, Campus Museum Contributions No. 5, p. 1-19.

Elders, W.A., and Sass, J.H., 1988, The Salton Sea scientific drilling project – Its scientific significance: Journal of Geophysical Research, v. 93, p. 12,953-12,968.

Elders, W.A., Rex, R.W., Meidav, T., Robinson, P.T., and Biehler, S., 1972, Crustal spreading in southern California – The Imperial Valley and the Gulf of California formed by rifting apart of a continental plate: Science, v. 178, p. 15-24.

Elders, W.A., Bird, D.K., Williams, A.E., and Schiffman, P., 1984, Hydrothermal flow regime and magmatic heat source of the Cerro Prieto geothermal system, Baja California, Mexico: Geothermics, v. 13, p. 27-47.

Fisher, R.V., and Schmincke, H.-U., 1984, Pyroclastic rocks: Berlin, Springer-Verlag, 472 p.

Folk, R.L., 1968, Petrology of sedimentary rocks: Austin, Texas, Hemphill's Book Store, 170 p.

Friedman, I., and Obradovich, J., 1981, Obsidian hydration dating of volcanic events: Quaternary Research, v. 16, p. 37-47.

Fuis, G.S., and Kohler, W.M., 1984, Crustal structure and tectonics of the Imperial Valley region, California *in* The Imperial basin – tectonics, sedimentation, and thermal aspects (C.A. Rigby, editor): Society of Economic Paleontologists and Mineralogists, Pacific Section publication, p. 1-13.

Grindley, G.W., and Browne, P.R.L., 1976, Structural and hydrologic factors controlling the permeability of some hot-water geothermal fields: United Nations Symposium on Development and Use of Geothermal Resources, 2nd, San Francisco, California, 20-29 May, 1975, Proceedings, p. 377-386.

Helgeson, H.C., 1968, Geologic and thermodynamic characteristics of the Salton Sea geothermal system: American Journal of Science, v. 266, p. 129-166.

Herzig, C.T., and Jacobs, D.C., 1994, Cenozoic volcanism and two-stage extension in the Salton trough, southern California and northern Baja California: Geology, v. 22, p. 991-994.

Herzig, C.T., Mehegan, J.M., and Stelting, C.E., 1988, Lithostratigraphy of the State 2-14 borehole, Salton Sea Scientific Drilling Project: Journal of Geophysical Research, v. 93, p. 12,969-12,980.

Hulen, J.B., and Sibbett, B.S., 1982, Sampling and interpretation of drill cuttings from geothermal wells: Society of Professional Well Log Analysts, Reprint Volume, p. IV3-IV54.

Hulen, J.B., and Pulka, F.S., 2001, Newly-discovered, ancient extrusive rhyolite in the Salton Sea geothermal field, Imperial Valley, California – Implications for reservoir characterization and duration of volcanism in the Salton trough: Stanford University, 26th Workshop on Geothermal Reservoir Engineering, Proceedings, 10 p.

Hulen, J.B., Kaspereit, D., Norton, D.L., Osborn, W., and Pulka, F.S., 2002, Refined conceptual modeling and a new resource estimate for the Salton Sea geothermal field, Imperial Valley, California: Geothermal Resources Council, Transactions, v. 26, p. 29-36.

Hulen, J.B., Norton, D.L., Moore, J.N., Osborn, W., van de Putte, T., and Kaspereit, D., 2003, The role of sudden dilational fracturing in evolution and mineralization of the southwestern Salton Sea geothermal system, California: Stanford University, 28th Workshop on Geothermal Reservoir Engineering, Proceedings, 25 p.

Irvine, P., 1983, Structural geology of the Salton Sea area: Unocal, Geothermal Division, Internal Report, 12 p.

Karig, D.E., and Jensky, W., 1972, The proto-Gulf of California: Earth and Planetary Science Letters, v. 127, p. 169-174.

Kasameyer, P.W., Younker, L.M., and Hanson, J.M., 1984, Development and application of a hydrothermal model for the Salton Sea geothermal field, California: Geological Society of America Bulletin, v. 95, p. 1242-1252.

Knapp, R.B., and Knight, J.E., 1977, Differential thermal expansion of pore fluids – Fracture propagation and microearthquake production in hot pluton environments: Journal of Geophysical Research, v. 82, p. 2515-2522.

Lachenbruch, A.H., Sass, J.H., and Galanis, S.P., 1985, Heat flow in southernmost California and the origin of the Salton Trough: Journal of Geophysical Research, v. 90, p. 6709-6736.

Lonsdale, P., 1989, Geology and tectonic history of the Gulf of California *in* The eastern Pacific ocean and Hawaii (E.L Winterer, D.M. Hussong, and R.W. Decker, editors): Geological Society of America, The Geology of North America, v. "N", p. 499-521.

Maher, J.C., 1964, Logging drill cuttings: Oklahoma Geological Society Guidebook XIV, 48 p.

McDowell, S.D., 1980, Authigenic layer silicate minerals in borehole Elmore 1, Salton Sea geothermal field, California, U.S.A.: Contributions to Mineralogy and Petrology, v. 74, p. 293-310.

McKibben, M.A., an Elders, W.A., 1985, Fe-Zn-Cu-Pb mineralization in the Salton Sea geothermal system, Imperial Valley, California: Economic Geology, v. 80, p. 539-559.

McKibben, M.A., and Hardie, L.A., 1997, Ore-forming brines in active continental rifts *in* Geochemistry of hydrothermal ore solutions, 3rd edition (H.L. Barnes, editor): New York, John Wiley, p. 877-935.

McKibben, M.A., Williams, A.E., and Okubo, S., 1988, Metamorphosed Plio-Pleistocene evaporites and the origin of hypersaline brines in the Salton Sea geothermal system, California – Fluid-inclusion evidence: Geochimica et Cosmochimica Acta, v. 52, p. 1047-1056.

McKibben, M.A., Andes, J.P., Jr., and Williams, A., 1989, Active ore formation at a brine interface in metamorphosed deltaic lacustrine sediments – The Salton Sea geothermal system, California: Economic Geology, v. 83, p. 511-523.

Merriam, R.; and Bandy, O.L., 1965, Source of upper Cenozoic sediments in the Colorado delta region: Journal of Sedimentary Petrology, v. 35, p. 911-916.

Moore, D.G., 1973, Plate-edge deformation and crustal growth, Gulf of California structural province: Geological Society of America Bulletin, v. 84, p. 1883-1906.

Moore, J.N., and Adams, M.C., 1988, Evolution of the thermal cap in two wells from the Salton Sea geothermal system, California: Geothermics, v. 17, p. 695-710.

Mrlik, R., and Strobel, C.J., 1986, Salton Sea project resource feasibility report, Imperial Valley district: Unocal, Geothermal Division, Internal Report, 167 p.

Muffler, L.J.P., and Doe, B.R., 1968, Composition and mean age of detritus of the Colorado River delta in the Salton trough, southeastern California: Journal of Sedimentary Petrology, v. 38, p. 384-399.

Muffler, L.J.P., and White, D.E., 1968, Origin of CO_2 in the Salton Sea geothermal system, southeastern California, U.S.A. *in* Genesis of mineral and thermal waters: Prague, International Geological Congress, v. 17, session XXIII, p. 185-194.

Muffler, L.J.P., and White, D.E., 1969, Active metamorphism of Upper Cenozoic sediments in the Salton Sea geothermal field and the Salton trough, California: Geological Society of America Bulletin, v. 80, p. 157-182.

Muramoto, F.S., and Elders, W.A., 1984, Correlation of wireline log characteristics with hydrothermal alteration and other reservoir properties of the Salton Sea and Westmoreland geothermal fields, Imperial Valley, California, U.S.A.: Los Alamos National Laboratory Report LA-10128-MS, 99 p.

Newmark, R.L., Kasameyer, P.W., Younker, L.W., and Lysne, P., 1988, Shallow drilling in the Salton Sea region – The thermal anomaly: Journal of Geophysical Research, v. 93, p. 13,005-13,024.

Norton, D.L., 1979, Transport phenomena in hydrothermal systems – The redistribution of chemical components around cooling magmas: Bulletin de Mineralogie, v. 102, p. 471-486.

Norton, D.L., 1982, Fluid and heat transport phenomena typical of copper-bearing pluton environments *in* Advances in geology of the porphyry copper deposits, southwestern North America (S.R. Titley, ed.): Tucson, University of Arizona Press, p. 59-72.

Norton, D.L., 1984, The theory of hydrothermal systems: Annual Review of Earth and Planetary Sciences, v. 12, p. 155-177.

Norton, D.L., and Dutrow, B.L., 2001, Complex behavior of magma-hydrothermal processes – Role of supercritical fluid: Geochimica et Cosmochimica Acta, v. 65, p. 4009-4017.

Norton, D.L., and Hulen, J.B., 2001, Preliminary numerical analysis of the magma-hydrothermal history of The Geysers geothermal system, California: Geothermics, v. 30, p. 211-234.

Osborn, W.L., 1989, Formation, diagenesis, and metamorphism of sulfate minerals in the Salton Sea geothermal system, California: University of California, Riverside, M.S. Thesis, 175 p.

Pickett, G.R., 1977, Resistivity, radioactivity, and acoustic logs *in* Subsurface geology – Petroleum, mining, construction (4th edition, L.W. Leroy and D.O. LeRoy, compilers): Colorado School of Mines, p. 304-336.

Reed, M.J., 1975, Geology and hydrothermal metamorphism in the Cerro Prieto geothermal field, Mexico: United Nations Symposium on Development and Use of Geothermal Resources, 2nd, San Francisco, California, 20-29 May, 1975, Proceedings, p. 539-547.

Rex, R.W., 1983, The origin of brines of the Imperial Valley, California: Geothermal Resources Council, Transactions, v. 7, p. 321-324.

Rex, R.W., 1985, Temperature-chlorinity balance in the hypersaline brines of the Imperial Valley, California *in* International symposium on geothermal energy (Proceedings; C. Stone, editor): Geothermal Resources Council Special Paper, p. 351-356.

Robinson, P.T., Elders, W.A., and Muffler, L.J.P., 1976, Quaternary volcanism in the Salton Sea geothermal field, Imperial Valley, California: Geological Society of America Bulletin, v. 87, p. 347-360.

Rook, S.H., and Williams, G.C., 1942, Imperial carbon dioxide field: California Division of Oil and Gas, Summary of Operations, Oil Fields, July-December 1942, v. 28, p. 12-33.

Schriener, A., Jr., 2001, Informal guidebook for Geothermal Resources Council Annual Meeting fieldtrip, geology and geothermal systems of the Salton Trough.

Scholle, P.A., 1979, A color illustrated guide to constituents, textures, cements, and porosities of sandstones and associated rocks: American Association of Petroleum Geologists, Memoir 28, 201 p.

Sibson, R.H., 1986, Brecciation processes in fault zones—Inferences from earthquake rupturing: Pure and Applied Geophysics, v.124, p. 159-175.

Skinner, B.J., White, D.E., Rose, H.J., and Mays, R.E., 1967, Sulfides associated with the Salton Sea geothermal brine: Economic Geology, v. 62, p. 316-330.

Smith, R.L., and Shaw, H.R., 1979, Igneous-related geothermal systems *in* Assessment of geothermal resources of the United States – 1975 (L.J.P. Muffler, editor): U.S. Geological Survey Circular 790, p. 12-17.

Suemnicht, G., Irvine, P., and Copp, J., 1984, Geologic summary of the Salton Sea field: Unocal, Geothermal Division, Internal Memorandum.

Sykes, G., 1937, The Colorado delta: American Geographic Society, Special Publication 19, p. 108-123.

Sylvester, A.G., 1988, Strike-slip faults: Geological Society of America Bulletin, v. 100, p. 1666-1703.

Tewhey, J.D., 1977, Geologic characteristics of a portion of the Salton Sea geothermal field: Lawrence Livermore Laboratory, Report UCRL-52267, 51 p.

van de Kamp, P.C., 1973, Holocene continental sedimentation in the Salton basin, California – A reconnaissance: Geological Society of America Bulletin, v. 84, p. 827-848.

White, D.E., Anderson, E.T., and Grubbs, D.K., 1963, Geothermal brine well – Mile-deep drill hole may tap ore-bearing magmatic waters and rocks undergoing metamorphism: Science, v. 139, p. 919-922.

Williams, A.E., and McKibben, M.A., 1989, A brine interface in the Salton Sea geothermal system, California: Fluid-geochemical and isotopic characteristics: Geochimica et Cosmochimica Acta, v. 53, p. 1905-1920.

Willis, G.F., and Tosdal, R.M., 1992, Formation of gold veins and breccias during dextral strike-slip faulting in the Mesquite mining district, southeastern California: Economic Geology, v. 87, p. 2002-2022.

Wohletz, K.H., 1986, Explosive magma-water interactions – Thermodynamics, explosion mechanisms, and field studies: Bulletin of Volcanology, v. 48, p. 245-264.

Wohletz, K.H., and Heiken, G., 1992, Volcanology and geothermal energy: Berkeley, University of California Press, 432 p.

Younker, L.W., Kasameyer, P.K., and Tewhey, J.D., 1982, Geological, geophysical, and thermal characteristics of the Salton Sea geothermal field, California: Journal of Volcanology and Geothermal Research, v. 12, p. 221-258.